International Journal of Innovative Computing, Information and Control
Volume **11**, Number **4**, August **2015**

 ISSN 1349-4198
pp. 1399–1410

PERFORMANCE COMPARISON OF INVERTER CONTROL TECHNIQUES FOR AN AXIAL POSITIONING SYSTEM: USING PM LINEAR SYNCHRONOUS ACTUATOR IN MAGNETICALLY SATURATED STATE

Ines Ben Salem and Lilia El Amraoui

Research Unit: Signals and Mechatronic Systems
Ecole Nationale d'ingénieurs de Carthage
Charguia 2, 2035 Tunis-Carthage, Tunisia
ines_bensl@yahoo.fr

Received October 2014; revised March 2015

Abstract. *This paper presents performance comparison between two inverter control techniques: PWM control and Direct Voltage Control (DVC). They are applied for a Permanent Magnet Linear Tubular Synchronous Actuator (PMLTSA) drive fed, to control instantaneous thrust and to ensure plunger position accuracy in magnetically saturated state. A dynamic modelling of the studied actuator is applied under magnetic nonlinearities. Then, an autopilot scheme is successfully implemented and simulated under MATLAB®/Simulink environment using the studied control techniques. Simulation results present large differences between the studied control strategies and prove the excellent performance of DVC approach, compared to PWM control technique.*
Keywords: PM linear synchronous actuator, Direct voltage control, Position control, Magnetic saturation, PWM

1. **Introduction.** The control of electrical machines records more and more increasing progress [1]. This progress is linked to evolution in numerical technique fields and performances are reached by components of power electronics [2].

In AC motors family, PM Synchronous Motor (PMSM) takes good place and becomes now widely used in various industrial applications [4]. Its advantages include high torque to current ratio, large power to weight ratio, higher efficiency and robustness. These important factors cannot hide some serious limits of the PMSM, like nonlinearity of the developed torque due to magnetic saturations [5]. This nonlinearity can introduce undesirable fluctuations on transient torque in heavy load operating points. This nonlinearity can also cause fails in the control scheme and constrain the system to stop, if the coupling effect between current components appears during transient dynamics [3,6].

The drive system plays an important role to control this nonlinearity. It should enable the drive to follow any reference function taking account of the effects of the load impact, the saturation variation and the parameter sensitivities [7-9].

In this paper, a control method based on Direct Voltage Control (DVC) strategy is compared to a PWM control technique. They are applied for a PM Linear Tubular Synchronous Actuator (PMLTSA) drive fed [10,11].

The aim of this work is to control force and plunger position of the actuator taking account of the magnetic nonlinearity effects and the load impacts on the dynamic behavior of the actuator.

For the actuator supply, we use three-phase Voltage Source Inverter (VSI) with current control levels. A closed-loop control system is considered to ensure plunger position and speed accuracy.

This paper is composed of four parts. Firstly, a brief description of the studied actuator and its dynamic modelling are presented. Secondly, the theoretical background of the inverter control techniques is summarized. Thirdly, closed control loops related to currents, plunger speed and position are applied to the dynamic modelling of the actuator. Finally, simulation results are discussed and compared.

2. Dynamic Modelling of the Actuator.

2.1. **Actuator description.** The studied actuator is a three phase tubular PM linear synchronous one equipped with quasi-halbach magnetization and modular stator structure. It is composed of 9 stator slots and 10 armature poles. The three stator armature windings are shifted from each other by a distance of $2\tau_p/3$, with τ_p the half pole pitch. Figure 1 presents the half cross section of the actuator structure. The parameter dimensions are presented in Table 1.

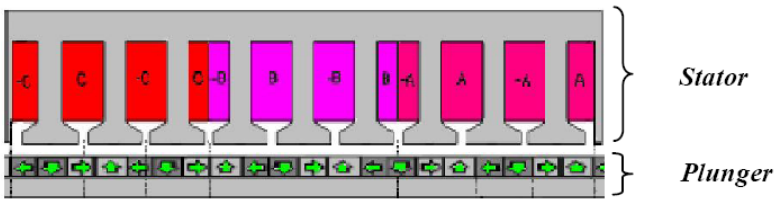

FIGURE 1. Half cross section of a PMLTSA structure

TABLE 1. Specifications and actuator parameters

Specifications	***Parameter value***
Resistor	$R_s = 0.6(\Omega)$
Pole pitch	$\tau_p = 10(\text{mm})$
plunger weight	$M = 4.5(\text{kg})$
Friction force coefficient	$f_v = 30(\text{N})$
Maximum load force	$F_l = 1500(\text{N})$
DC voltage supply	$V_{DC} = 42(\text{V})$
Sampling time	$T_d = 10(\mu\text{s})$
Modulation period	$T_s = 0.1(\text{ms})$
Maximum force	$F_{\max} = 5(\text{kN})$

2.2. **Dynamic modelling.** The dynamic modelling of the PMTLSA is presented as a coupling of electric, magnetic and mechanic models as shown in Figure 2. It takes account of the nonlinear magnetic effects and it develops sinusoidal electromotive force.

For an accurate computation of F_{em}, E and L_{abc}, a 2D axisymmetric Finite Element Model (FEM) is developed under PC-Opera® software environment. The waves of these curves are computed, according to different current densities and over one pole pitch.

These 3D finite element results are then stored on 2D Lookup tables under MATLAB® /Simulink environment using 3D response areas. Then, they are injected on the dynamic model of the actuator.

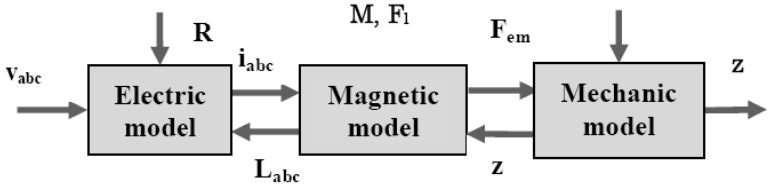

FIGURE 2. Synoptic diagram of the actuator model coupling

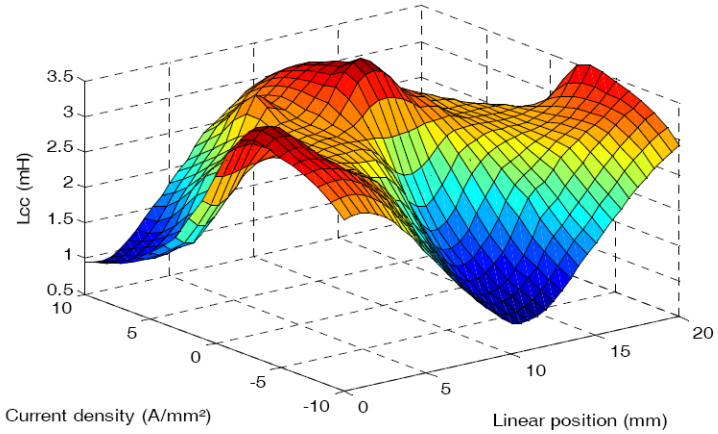

FIGURE 3. Response area of self inductance L_{cc}

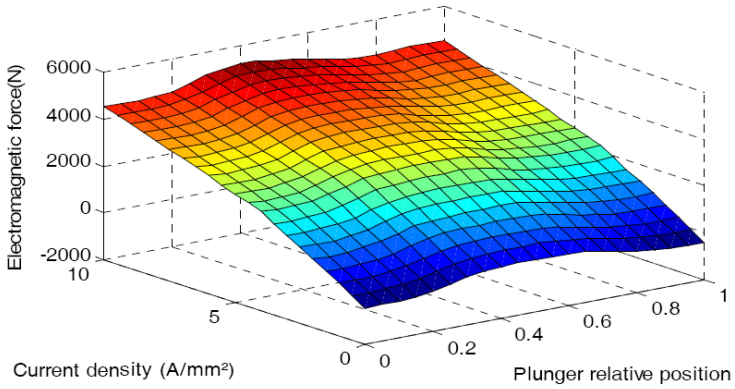

FIGURE 4. Response area of electromagnetic force F_{em}

To ensure the continuity between the different points of 3D curves, a linear interpolation function is applied. Figures 3 and 4 present respectively the response area of the self inductance (L_b) and the electromagnetic force (F_{em}).

The dynamic modelling of the actuator is expressed with Equations (1), (2), (3) and (4).

$$\frac{d}{dt}\begin{pmatrix} i_{abc} \\ z^2 \end{pmatrix} = \begin{pmatrix} [L_{abc}]^{-1}\,[v_{abc} - Ri_{abc} - e_{abc}] \\ \frac{1}{M}(F_{em} - (F_v \frac{d}{dt} z + F_l)) \end{pmatrix} \tag{1}$$

with:

$$e_{abc} = \begin{pmatrix} e_a \\ e_b \\ e_c \end{pmatrix} = -\frac{dz}{dt}.N_p\psi_{pm}\begin{pmatrix} \sin(N_p z) \\ \sin(N_p z + \frac{2\pi}{3}) \\ \sin(N_p z + \frac{4\pi}{3}) \end{pmatrix} \tag{2}$$

$$[L_{abc}] = \begin{bmatrix} L_a & 0 & 0 \\ 0 & L_b & 0 \\ 0 & 0 & L_c \end{bmatrix} \tag{3}$$

$$F_{em}(i,z) = \sum_{k=a,b,c} \frac{d\psi_k}{dz} i_k \mid_{i_k=cte} \tag{4}$$

v_{abc} is the actuator model input. i_{abc} and z are at the same time, the state spaces and the model outputs. Nomenclatures of the different abbreviations are presented in Table 2.

TABLE 2. Nomenclatures

Symbol	***Description***
N_p	*Electrical position constant*
τ_p	*Plunger pole pitch*
v_{abc}	*Supply voltage vector*
$\bar{v}_{ref}$	*Voltage reference vector*
i_{abc}	*Current vector*
$\bar{i}_{ref}$	*Current reference vector*
e_{abc}	*Electromotive force vector*
ψ_{pm}	*Maximum value of PM flux*
ψ_k	*Flux in phase k, with* $k = \{a, b, c\}$
R	*Statoric resistor matrix*
L_{abc}	*Statoric inductance matrix*
F_{em}	*Electromagnetic force generated by the actuator*
F_{ref}	*Reference force*
F_v	*Friction force coefficient*
F_l	*Load force*
z_{ref}	*Reference position*
z	*Plunger position*
M	*Plunger weight*
τ_m	*Mechanic time constant*
K_{pp}	*Position controller factor*
K_{pv}, K_{Iv}	*Speed controller factors*
K_p, K_I	*Current controller factors*

3. **Background of the Inverter Control Strategies.** The inverter source supplying the actuator is associated to a current control sub-system for a force control purpose.

3.1. **VSI modelling.** For an ideal three phases VSI, the voltage vector v_{abc} is strictly dependent on the DC bus voltage V_{DC} and the logical states of the three switches c_1, c_2 and c_3 (5). The two switching commands of each leg are complementary. Therefore, only three independent variables are sufficient to define the inverter states. These variables are here represented by three Boolean variables c_1, c_2 and c_3, where $c_1 = \bar{c}_4$, $c_2 = \bar{c}_5$ and

$c_3 = \bar{c}_6$.

$$v_{abc} = \begin{bmatrix} v_a \\ v_b \\ v_c \end{bmatrix} = \frac{V_{DC}}{3} \begin{bmatrix} 2 & -1 & -1 \\ -1 & 2 & -1 \\ -1 & -1 & 2 \end{bmatrix} \begin{bmatrix} c_1 \\ c_2 \\ c_3 \end{bmatrix} \tag{5}$$

3.2. **The sinusoidal PWM control strategy.** The sinusoidal PWM control technique is the most used for industrial converters. The basic principle of the PWM technique involves the comparison of triangular wave frequency with the fundamental frequency of a sinusoidal modulating wave [2,6].

In this study, the voltage inverter is controlled with a current control sub-system, so a PI current controller is used for each phase of the actuator. This PI control bloc provides a saturated voltage reference vector. The associated integral action is limited with an optimal algorithm.

3.3. **The DVC control strategy.** The DVC strategy is based on the space vector PWM control strategy. It can operate in three different modes: position control, voltage control, and load control. It aims to follow one specific vector by the control low that respects the min (max) criterion [12-14].

In this case, the sampling time T_d is chosen to be N times smaller than the modulation period T_s, used by the space vector PWM control technique ($T_s = T_d N$).

The voltage reference vector $\bar{v}_{ref}$, provided by the PI current control loop, is expressed with Equation (6), where ζ is the reference voltage angle.

$$\overline{v}_{ref} = \frac{V_{ref}}{V_{DC}} e^{j\zeta} \tag{6}$$

The studied system is considered as a balanced one. The associated space vector in the Concordia reference frame work (d, q) is used.

In recurrent form, the voltage space vectors are expressed with equations system (7), Figure 5 and Figure 6.

$$\begin{cases} \bar{v}_k = \sqrt{\frac{2}{3}} V_{DC} e^{j\theta_{vk}} & \text{for } k = \{1, 2, \ldots, 6\} \\ \bar{v}_k = 0 & \text{for } k = \{0; 7\} \end{cases} \quad \text{with } \theta_{vk} = (k-1)\frac{\pi}{3} \tag{7}$$

The minimization process takes account of the two components ε_d and ε_q of the voltage error at the same time. As the voltage vector is constant during the considered interval time, the voltage error evolution can be expressed by $\bar{\varepsilon}$ (8). The adequate voltage vector is selected by solving the constraint (9).

$(n = 1, \ldots, 7)$ is an index to distinguish the effect of each voltage error on voltage vector.

$$\bar{\varepsilon}(n(t_k)) = \varepsilon_d + j\varepsilon_q = \bar{\varepsilon}(t_k) + T_d \left[\bar{v}_{ref}(t_k) - \bar{v}(n(t_k))\right] \tag{8}$$

$$\min_{n=1,\ldots,7}(\varepsilon(n)) = \min_{n=1,\ldots,7}(\max(|\varepsilon_d(n)|, |\varepsilon_q(n)|)) \tag{9}$$

The DVC structure can be summarized on three steps:

Step 1:

- voltage vector choice
- voltage error components computation
- saving of the maximum absolute value of these components,

Step 2: Iteration of the process is applied to the other voltage vectors,

Step 3:

- selection of the first one
- selecting the associated index voltage n.

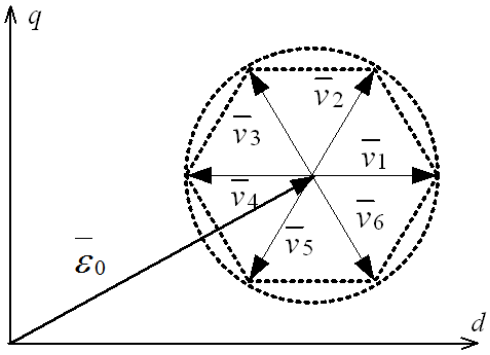

FIGURE 5. Reference voltage vectors in Concordia reference frame

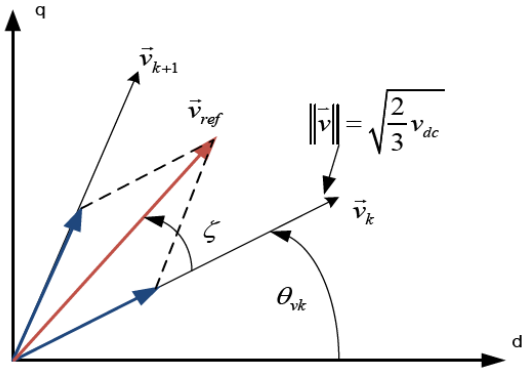

FIGURE 6. Inverter voltage vector in Concordia reference frame

4. **Closed Loop Control Structure.** For a current control purpose, two PI controllers are used in Concordia reference frame. Expression (10) and (Figures 7 and 8) present the current control strategy using an e.m.f compensation.

$$\bar{v}_{ref} = \left[K_p + \frac{K_I}{p}\right] [\bar{i}_{ref} - \bar{i}] + \bar{E} \tag{10}$$

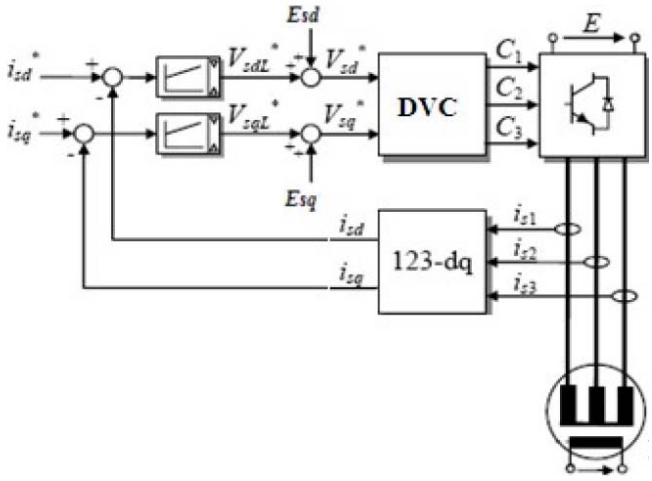

FIGURE 7. Synoptic diagram of the actuator current control strategy

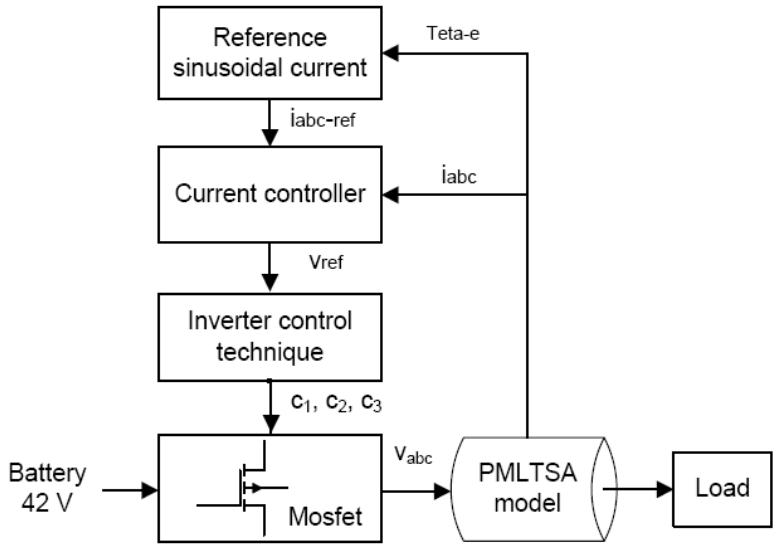

FIGURE 8. Synoptic diagram of the actuator current control scheme

For an instantaneous force control, a PID controller is used. It is expressed by Equation (11).

$$F_{ref} = \left[K_{pv} + \frac{K_{Iv}}{p}\right][z_{ref} - z]\, p \tag{11}$$

with $F_v \leq K_{pv} \leq \sqrt{F_{\max} M}$ and $K_{Iv} = \frac{K_{pv}}{\tau_m}$.

5. Simulation Results.

5.1. **Current control results.** The purpose of this section is to evaluate the performance of the proposed control techniques presented below. These approaches are implemented in the Simulink environment. They are tested to supply a PMLTSA working in autopilot mode and using a three phases VSI.

The same initial conditions are applied in these simulations cases, as well as, frequency, reference values and load. Two current levels chosen respectively in saturated and non saturated magnetic states ($I_{m1} = 5$A and $I_{m2} = 20$A) are tested for:

$$i_{ref}(t) = I_m \sin(N_p z) \text{ with } N_p = \pi/\tau_p \tag{12}$$

The actuator force load is considered as a linear function of the plunger speed v, with a maximum value of 1.5kN (13).

$$F_l = K.v \quad \text{with } K \text{ a constant value} \tag{13}$$

For the same simulation conditions, the sampling time used in simulation is $T_S = 0.1$ms for PWM and DVC control structure.

5.1.1. *Case of non saturated state.* The PMLTSA is initially running with a current reference level equal to $I_{m1} = 5$A, and under a load regime.

The dynamic force reaches 190N in the steady state in two cases. The best response time is followed with the DVC technique. It is less than 0.3ms. For the PWM technique, we have more than 0.5ms, Figures 9 and 11.

Also, for this low current level, successful results are confirmed by the good statoric current waveforms, (Figures 10 and 12).

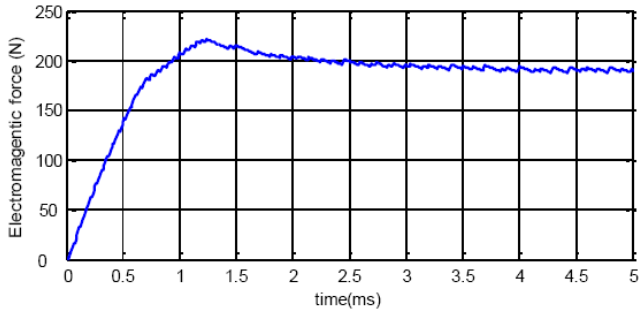

FIGURE 9. Dynamic force evolution with PWM control

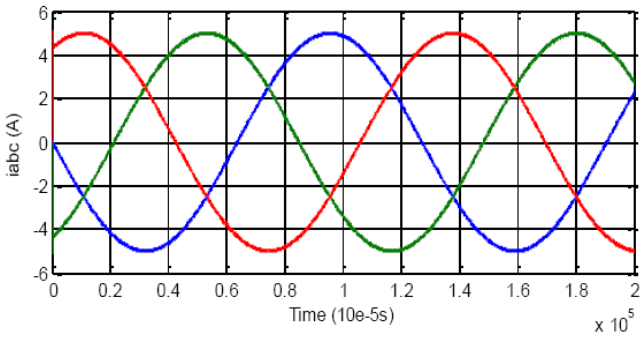

FIGURE 10. Current evolutions with PWM control

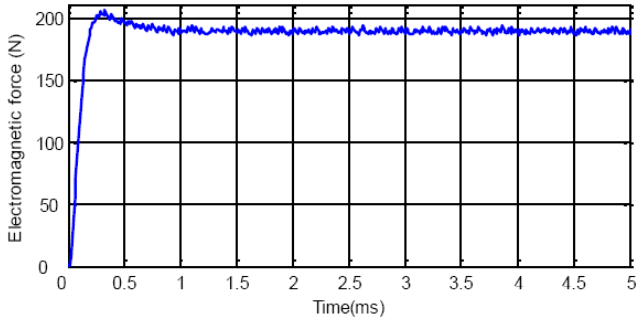

FIGURE 11. Dynamic force evolution with DVC control

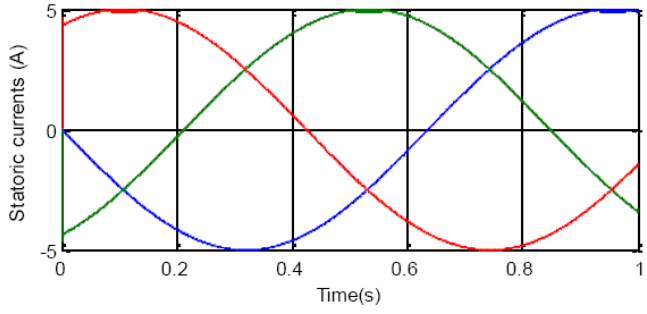

FIGURE 12. Current evolutions with DVC control

5.1.2. *Case of saturated state.* For $I_m = 20A$, with PWM control technique, same forces ripples are observed (Figure 13). In the steady state, the dynamic force is reaching 760N. These ripples are reduced with the DVC control technique and a quasi constant dynamic force is observed (Figure 15).

Concerning the response times, DVC technique has less than 0.5ms. For the second technique, this time is more than 1.5ms in the same simulation conditions.

For this high current level, the statoric current waveforms, obtained from the DVC technique (Figure 16), follow the reference current evolutions. With the PWM technique, current curves do not conform to the reference currents values, especially on the curve picks (Figure 14).

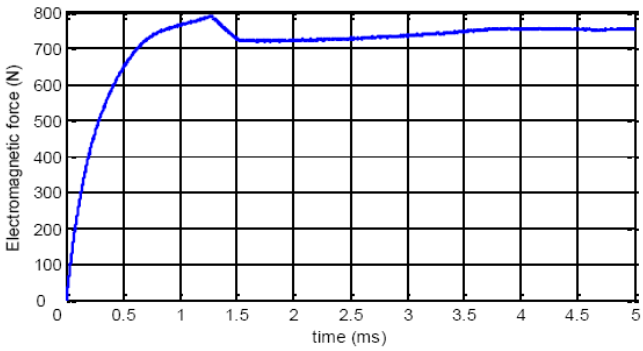

FIGURE 13. Dynamic force evolution with PWM control

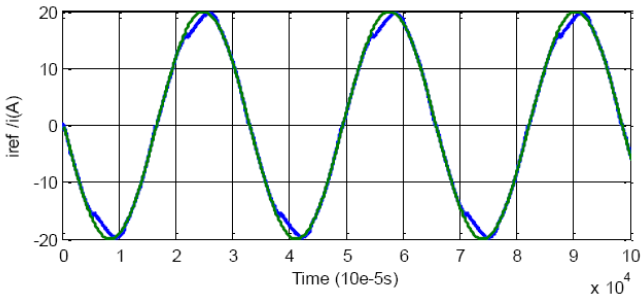

FIGURE 14. Currents evolutions with PWM control

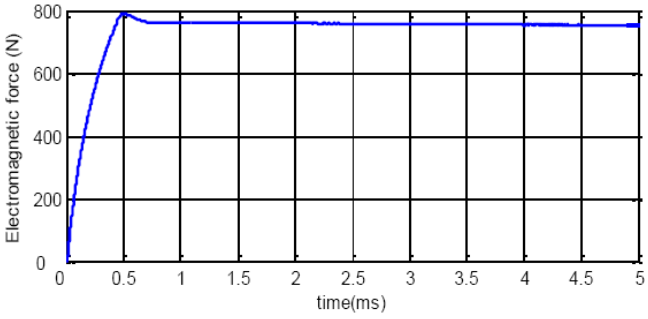

FIGURE 15. Dynamic force evolution with DVC control

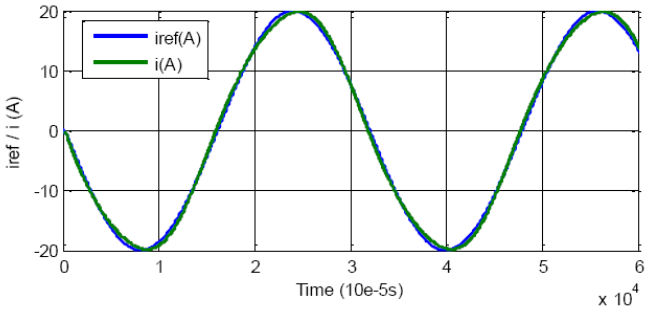

FIGURE 16. Currents evolutions with DVC control

These simulation results verify that the proposed strategies have a fast dynamic response and can effectively control the generated voltage under different linear or nonlinear loads with different degrees of accuracy. As shown, with these control techniques, the DVC one produces the best dynamic force and current characteristics, with minimum ripples and low response time. Therefore, it is used for the speed and plunger position control system.

5.2. **Speed and plunger position control results.** The purpose of this section is to evaluate the performances of the proposed speed and plunger position control structures, when a trapezoidal reference speed is applied. A force load variation of 50% is generated at $t = 3$s. Figure 17 presents the superposition of the speed and the speed reference. A 10% variation of the generated speed is observed at $t = 3$s.

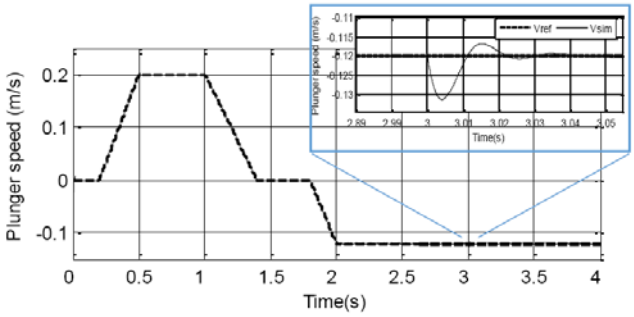

FIGURE 17. Plunger speed evolution

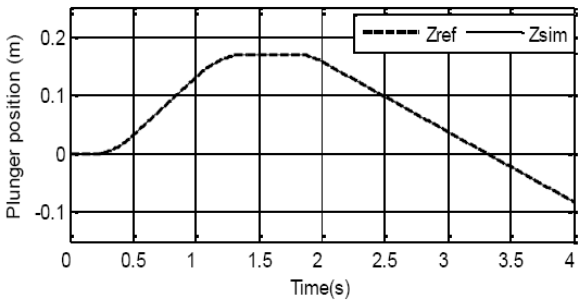

FIGURE 18. Plunger position evolution

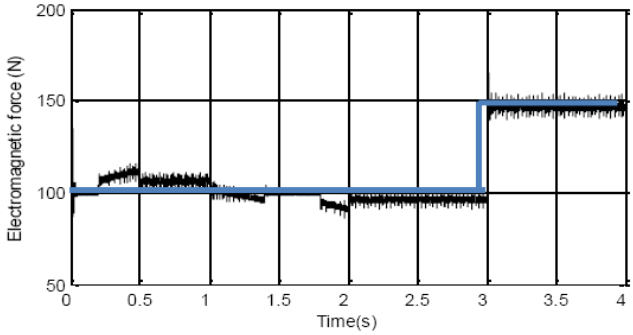

FIGURE 19. Electromagnetic force (black)/loaded force (gray)

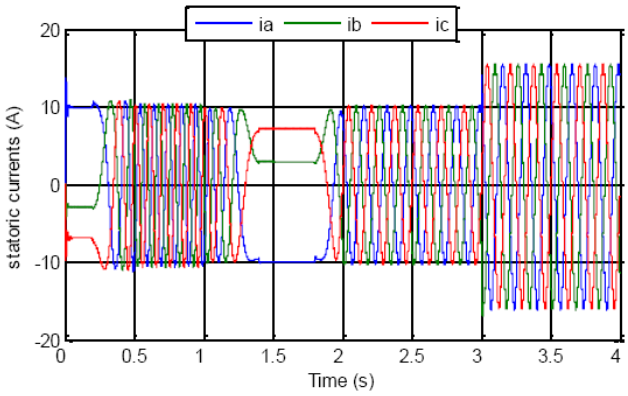

FIGURE 20. Statoric currents evolution

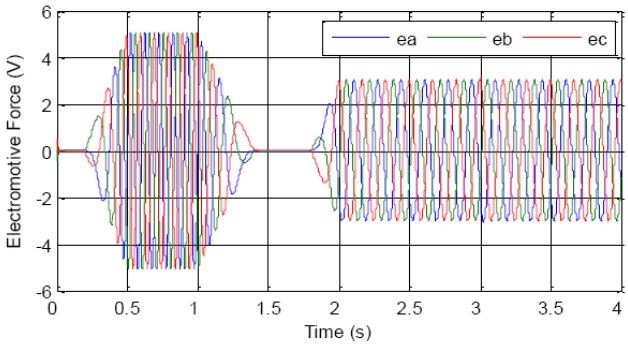

FIGURE 21. Electromotive forces evolution

6. **Conclusion.** This paper presents performance comparison between two control techniques of a voltage source inverter: PWM and DVC techniques. This inverter is used to supply a PM linear synchronous actuator, used to actuate a high dynamic positioning application. A nonlinear dynamic modelling of this actuator is presented, taking account of the magnetic nonlinearities of the actuator structure.

The simulation results developed under Simulink environment show the difference between the studied control techniques. Force ripples and response times are observed on the dynamic simulated forces, compared for two references of current. The obtained results prove that in linear magnetic conditions, a good accuracy is observed in currents and force evolutions. For nonlinear magnetic conditions, current curves present ripple with PWM technique. With DVC technique, currents are conforming to impose references.

The studied control techniques satisfy the tracked objective, but DVC approach is the most suitable for the inverter control at saturated and non saturated states. The latter technique presents especially these advantageous:

- Do not require a very high number of commutations to provide good accuracy minimizing the switching losses in the inverter.
- Working with constant switching time avoids the use of high quality power electronic components. Inverters based on classical transistors can be then used.

In closed loop control structure and using the DVC, the developed work ensures a performed axial dynamic positioning with instantaneous thrust control, as well as a high speed and position accuracy.

REFERENCES

[1] A. R. Ghafari-Kashani, J. Faiz and M. J. Yazdanpanah, Integration of non-linear H_∞ and sliding mode control techniques for motion control of a permanent magnet synchronous motor, *Electric Power Applications, IET*, vol.4, 2010.

[2] A. Emadi, *Handbook of Automotive Power Electronics and Motor Drives*, Taylor & Francis Group, LLC, 2005.

[3] T. Sebastian and G. R. Slemon, Operating limits of inverter-driven permanent magnet motor drives, *IEEE Trans. Industry Applications*, vol.23, no.2, 1987.

[4] J. F. Gieras and Z. J. Piech, *Linear Synchronous Motors: Transportation and Automation Systems*, CRC Press, Boca Raton, 2000.

[5] J. Wang and D. Home, Design optimisation of radically magnetized, iron-cored, tubular permanent magnet machines and drives system, *IEEE Trans. Magnetics*, vol.40, no.5, 2004.

[6] I. Ben Salem, L. El Amraoui Ouni, M. Benrejeb, F. Gillon and P. Brochet, Flux linkage approach used for phase inductance calculation of a tubular linear PM synchronous actuator, *International Review of Electrical Engineering (IREE)*, vol.6, no.5, 2011.

[7] Y.-W. Zhu and Y.-H. Cho, Thrust ripples suppression of permanent magnet linear synchronous motor, *IEEE Trans. Magnetics*, vol.43, no.6, 2007.

[8] F. Cupertino, G. Pellegrino, P. Giangrande and L. Salvatore, Sensorless position control of permanent-magnet motors with pulsating current injection and compensation of motor end effects, *IEEE Trans. Industry Applications*, vol.47, 2011.

[9] A. Narayanaswamy, P. R. Iyer and J. Zhu, Interactive modelling and simulation of a six step continuous current mode inverter fed PMSM drive using Simulink, *IEEE Trans. Magnetics*, 2006.

[10] I. Ben Salem, L. El Amraoui Ouni, M. Benrejeb, F. Gillon and P. Brochet, Performance comparison of inverter control techniques used for the supply of a linear PM synchronous actuator, *International Aegean Conference on Electric Machines and Power Electronics & Electromotion Joint Conference*, Istanbul, Turkey, 2011.

[11] C.-C. Sung and Y.-S. Huang, Based on direct thrust control for linear synchronous motor systems, *IEEE Trans. Industrial Electronics*, vol.56, no.5, 2009.

[12] A. Hmidety, R. Dhifaoui and O. Hasnaoui, Development, implementation and experimentation on a dSPACE DS1104 of a direct voltage control scheme, *Journal of Power Electronics*, vol.10, no.5, 2010.

[13] H. Geng, D. Xu, B. Wu and W. Huang, Direct voltage control for a stand-alone wind-driven self-excited induction generator with improved power quality, *IEEE Trans. Power Electronics*, vol.99, 2011.

[14] S. G. Buja and M. P. Kazmierkowski, Direct torque control of PWM inverter-fed AC motors a survey, *IEEE Trans. Industrial Electronics*, vol.51, no.4, 2004.